Geobiology (2004), **2**, 121–132

TEM evidence for eukaryotic diversity in mid-Proterozoic oceans

EMMANUELLE J. JAVAUX[1], ANDREW H. KNOLL[2] AND MALCOLM R. WALTER[3]

[1]*Department of Astrophysics, Geophysics and Oceanography, University of Liège, Sart-Tilman 4000 Liège, Belgium*
[2]*Department of Organismic and Evolutionary Biology, Harvard University, Cambridge, Massachusetts 02138, USA*
[3]*Australian Centre for Astrobiology, Macquarie University, Sydney, NSW 2109, Australia*

ABSTRACT

Biomarker molecular fossils in 2770 Ma shales suggest that the Eucarya diverged from other principal domains early in Earth history. Nonetheless, at present, the oldest fossils that can be assigned to an extant eukaryotic clade are filamentous red algae preserved in ca. 1200 Ma cherts from Arctic Canada. Between these records lies a rich assortment of potentially protistan microfossils. Combined light microscopy, scanning electron microscopy, and transmission electron microscopy on 1500-1400 Ma fossils from the Roper Group, Australia, and broadly coeval rocks from China show that these intermediate assemblages do indeed include a moderate diversity of eukaryotic remains. In particular, preserved cell wall ultrastructure, observed using transmission electron microscopy (TEM), can help to bridge the current stratigraphic gap between the unambiguous eukaryotic morphologies of later Proterozoic assemblages and molecular biomarkers in much older rocks.

Received 02 March 2004; accepted 07 June 2004

Corresponding author: Dr Emmanuelle J. Javaux. Tel.: 32 4 366 9763; fax: 32 4 366 9746; e-mail: ej.javaux@ulg.ac.be

INTRODUCTION

When did eukaryotic organisms begin to diversify in the oceans? Phylogenies based on small subunit rRNA genes (Pace, 1997) and whole genomes (House & Fitz-Gibbon, 2002) suggest that eukaryotes diverged from other domains early in Earth history, an inference supported by the presence of C_{28-30} steranes in 2.7 billion year old (Ga) shales (Brocks *et al.*, 1999). However, modern eukaryotic cell biology and, hence, recognizable fossils of eukaryotic organisms, could significantly postdate the gene divergences implied by molecular phylogenies. The late Archean biomarkers indicate the presence of cells able to synthesize eukaryotic sterols (prokaryotes are not known not make sterols with the particular side chain modification indicated by the molecular fossils; Pearson *et al.*, 2003), but not necessarily cells with a nucleus, cytoskeleton, endomembranes, or organelles. Fossils of red, green and xanthophyte algae; testate amoebae; and other unambiguously eukaryotic organisms show that eukaryotic cells began to diversify no later than 1–1.2 Ga, well before anatomically complex animals spread through the oceans (e.g. Knoll, 1992; Xiao *et al.*, 1997; Butterfield, 2000, 2004; Javaux *et al.*, 2003; Porter *et al.*, 2003; for an alternative view see Cavalier-Smith, 2002). The challenge, then, is to connect the later Proterozoic record of recognizable crown group eukaryotes with older, more problematic fossils of possible stem taxa (either to the Eucarya as a whole or to major clades within the domain) and to integrate both with phylogenies based on comparative biology. Meeting this challenge requires palaeontological exploration for an extended range of eukaryotic phenotypes that includes ultrastructural and chemical records, as well as morphological remains. In this paper, we argue that preserved cell wall ultrastructure, observed using TEM, can help to bridge the current stratigraphic gap between the unambiguous eukaryotic morphologies of later Proterozoic assemblages and molecular biomarkers in much older rocks.

Previous studies of wall ultrastructure in fossil protists

The study of wall ultrastructure in acritarchs remains in its infancy. (Acritarchs are organic-walled microfossils of unknown biological affinities, with various morphospecies interpreted as cyanobacterial envelopes, spore walls of algae or heterotrophic protists, or even cysts or egg cases of multicellular organisms.) Until now, acritarch wall ultrastructure has been investigated only in a few species, nearly all much younger than those examined in this paper. The earliest TEM studies of

Proterozoic and Palaeozoic microfossils date from the late 1960s to early 1980s (e.g. Jux, 1968, 1971, 1977; Kjellström, 1968; Loeblich, 1970; Martin & Kjellström, 1973; Oehler, 1977; Peat, 1981). More recent work by Talyzina & Moczydlowska (2000) on Early Cambrian acritarchs revealed four structurally distinct types of vesicle walls. *Tasmanites tenellus* has a homogeneous electron-dense wall punctuated by pore canals, similar to the phycomata of some prasinophyte green algae. Acanthomorphic (process-bearing) microfossils display an electron-tenuous fibrous (*Archaeodiscina umbonulata*) or electron-dense homogeneous wall (*Globosphaeridium cerinum*, *Comasphaeridium brachyspinosum*, *Skiagia compressa*). *Leiosphaeridia* sp. shows a multilayered wall with an outer laminated layer resembling the trilaminar sheath structure (TLS) found in many chlorococcalean green algae, an intermediate tenuous homogeneous layer, and an internal dense homogeneous layer.

Arouri *et al.* (1999, 2000) studied the ultrastructure and chemistry of Neoproterozoic acritarchs from Australia, suggesting a dinoflagellate affinity for acanthomorph (process-bearing) species (*Alicesphaeridium*, *Tanarium* and species C2) with a multilayered, fibrillar wall and chlorophycean relationships for other taxa (*Multifronsphaeridium pelorium* and species A), whose walls preserve a laminated organization similar to the trilamellar structure (TLS) found in some extant green algae. Specimens of *Chuaria* and *Leiosphaeridia* sp. display a uni-layered electron-dense wall ultrastructure; *Tasmanites* sp. preserve a similar ultrastructure but perforated by numerous canals, again suggesting a prasinophyte green algae affinity. Both thinner-walled (0.5–2.5 μm) and thicker-walled (2.3–5.4 μm) specimens assigned to *Chuaria* from the Neoproterozoic Visingsö Group, Sweden, have a single-layered, electron-dense homogeneous wall (Talysina, 2000). Other chuarids from the late Neoproterozoic Pendjari Formation, West Africa, show a multilamellar ultrastructure with structures interpreted as pore canals (Amard, 1992). Interpreted chuarids from the Liulaobei Fomation in China (Steiner, 1997) display a variable wall structure ranging from massive to striate, multilayered walls in thick specimens with no or only local central cavity to single-layered amorphous wall in thinner-walled specimens with a large central cavity. Steiner (1997) interpreted these fossils as *Nostoc*-like prokaryotic colonies, although living nostocaleans do not tolerate fully marine environments. The Liulaobei remains could be cyanobacterial envelopes, but their phylogenetic relationship to either *Chuaria circularis* from its type locality or any extant taxon remains uncertain. Insofar as their systematic affinities cannot be established with confidence, these fossils cannot be used to establish the range of ultrastructures exhibited by prokaryotic vs. eukaryotic microorganisms.

Previous work on unambiguously eukaryotic acritarch wall ultrastructure, thus, shows that both acanthomophic and sphaeromorphic species can have multilayered or unilayered walls, with only *Tasmanites* spp. characterized by transverse canals, a characteristic of the phycoma (resting cysts) of some prasinophyte green algae. Canals reported by Jux (1971) in the wall of Palaeozoic genera *Baltisphaeridum* and *Peteinosphaeridum* are irregular in both shape and distribution and likely formed diagenetically, as also reported by Talyzina (2000).

Of course, complex wall ultrastructure can only be adduced as evidence for eukaryotic cell biology only if prokaryotic organisms do not form similar acetolysis-resistant walls (see review in Javaux *et al.*, 2003). Few bacteria make spores with a size, surface ornamentation, and preservation potential observed in Proterozoic acritarchs. A few bacteria, for example, the Myxobacteria (which are mostly terrestrial), have sporangioles (spore enclosing envelopes) up to 50 microns in diameter, but these are smooth walled structures of unknown chemical composition that are not known to survive in sediments. Although vegetative cells of Actinobacteria can be relatively large (a few microns) and form complex branching colonies, their spores are 0.5–2 or 3 μm in diameter and form chains. These spores can be ornamented but their rodlets, spines, warts, cristae, or hair-like tufts are nano-scale proteinaceous structures unlikely to survive in geological environments.

Cyanobacterial sheaths are more likely candidates for comparison with Proterozoic fossils. Spheroidal envelopes of coccoidal cyanobacterial colonies can exceed 100 microns in size, and these polysaccharide structures are commonly fossilized (e.g. Knoll & Calder, 1983; Bartley, 1996). Cyanobacterial envelopes do not display surface ornamentation, so only simple spheroidal fossils (leiosphaerids) bear comparison. These cyanobacterial envelopes, however, differ from protistan (unicellular eukaryotes) walls at the ultrastructural level, consisting of fibrous layers (Waterbury & Stanier, 1978; Fig. 1) quite distinct from any of the ultrastructures described in this paper (J. Waterbury, pers. comm., 2003).

Thus, existing data indicate that the structural complexity of eukaryotic cell walls can be preserved in ancient microfossils and distinguished from acetolysis-resistant structures formed by bacteria (Javaux *et al.*, 2003). This, in turn, suggests that ultrastructural features can provide evidence for eukaryotic affinities, even in older Proterozoic rocks, where morphology may be ambiguous.

MATERIALS AND METHODS

Most of the fossils treated here were recovered from carbonaceous shales of the early Mesoproterozoic Roper Group (Fig. 1), northern Australia. The Roper Basin is well-characterized in terms of sedimentary architecture (Abbott & Sweet, 2000) and is abundantly fossiliferous (Peat, 1981; Javaux *et al.*, 2001). Roper microfossil assemblages show an onshore-offshore pattern of decreasing abundance, declining diversity, and changing dominance (Javaux *et al.*, 2001). U-Pb SHRIMP analyses of zircons from an ash bed in the Mainoru Formation fix an age of 1492 ± 3 Ma for early Roper deposition (Page *et al.*, 2000). A 1429 ± 31 Ma Rb-Sr age for illite in dolomitic siltstones near the top of the succession is consistent with the

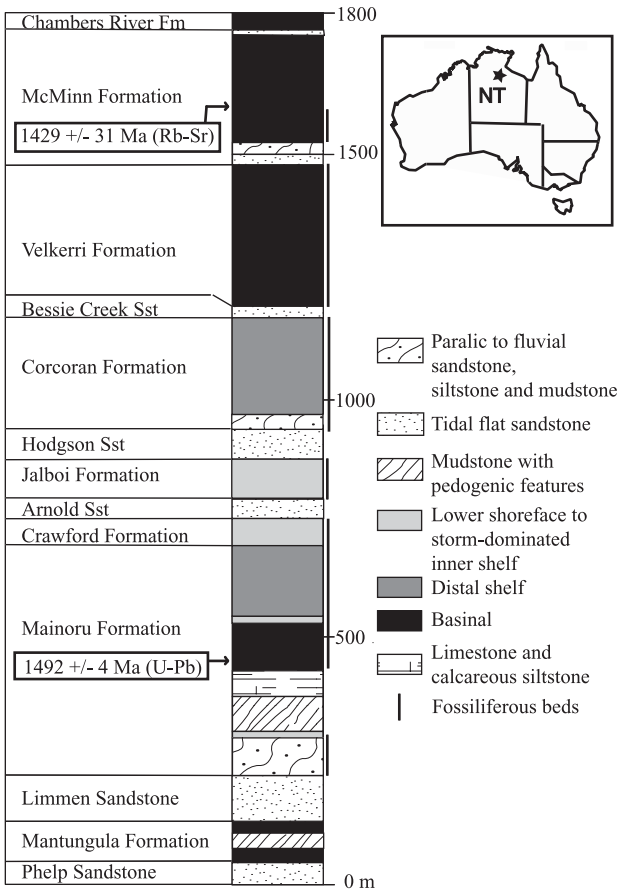

Fig. 1 Location and generalized stratigraphy of the Roper Group, northern Australia, showing stratigraphic distibution of facies and microfossils. Modified from Javaux *et al*. (2001).

zircon age, if less reliable (Kralik, 1982). Highly carbonaceous shales in basinal deposits of the Velkerri Formation, near the top of the Roper Group, also contain low abundances of steranes sourced by eukaryotic organisms (Summons *et al.*, 1988).

One highly ornamented fossil also treated here, *Shuiyousphaeridium macroreticulatum*, comes from shales of the Ruyang Group, northern China. Ruyang deposition is not well constrained by radiometric dates, but appears to be at least broadly coeval with Roper sedimentation. A *c.* 1000 Ma granite (U-Pb zircon date) intrudes the Ruyang succession, providing a minimum age for the group; moreover, abundant microdigitate precipitates and C-isotopic profiles that vary little from 0‰ in thick, overlying carbonates suggest that Ruyang shales are older than *c.* 1250 Ma (Xiao *et al.*, 1997). Ruyang shales share several distinctive taxa (species of *Tappania*, *Valeria*, and *Dictyosphaera*) with the Roper Group. Similar microfossil assemblages occur in the c.1.3 Ga Totta Formation, Siberia (Sergeev, pers. comm., 2002), and the poorly dated but broadly correlative Sanda Formation, Ganga Basin, India (Prasad & Asher, 2001).

Microfossils were extracted from shales using a modified palynological method involving slow hydrofluoric acid digestion with minimal agitation (Grey, 1999). Extracted fossils were mounted with eukitt plastic resin for light microscopy. For SEM, individual microfossils were picked from unmounted macerates and placed on glass coverslips glued onto aluminium stubs. Stubs were then coated with a 22 nm layer of gold-palladium. Scanning electron microscopy was carried out using a LEO 982 microscope at 5 KV.

For TEM, various preparation methods were tried and adapted, especially with regard to infiltration and polymerization times, microfossil manipulations and type of resin used. Microfossils were embedded in agar, dehydrated in a series of ethanol solutions, and then infiltrated with a mixture of propylene oxide/ethanol, followed by propylene oxide/epoxy resin, and then pure Epoxy. In a second method, individual microfossils were dehydrated in a series of ethanol solutions, and then infiltrated with ethanol/Spurr solution, followed by pure Spurr resin. Samples were then polymerized in an oven at 60 °C for at least 12 h. After verifying the proper orientation of individual microfossils, resin blocks were trimmed and cut into 50 nm thick ultrathin sections with a diamond knife. Sections were put on copper grids and observed under a Zeiss 10CA TEM at 80 KV. No staining was used as it was shown unnecessary in previous studies (Oehler, 1977; Talyzina *et al.*, 2000) and can be source of artifacts.

The 1.5–1.3 Ga microfossils are extremely well preserved morphologically and have undergone little thermal alteration, although some taphonomic changes have, of course, occurred due to burial compaction and biodegradation (removal of less resistant molecules such as proteins, nucleic acids and sugars). Determination of Thermal Alteration Index (TAI) from observation of acritarch colours (Batten, 1996) shows a range from 1/2 to 4 (yellow to orange brown), immature to early mature for the Roper group acritarchs, and early mature (orange brown to brown) for the Ruyang Group. Several ultrathin sections of two to three specimens of each species, and in some cases from different facies (Table 1), were examined and gave consistent results, showing particular wall ultrastructure for each species in relation to their biology and not to different taphonomies (preservation in different physico-chemical conditions) or to the preparation of specimens for TEM. Great care was taken in the interpretation of EM images to discard any artifacts possibly caused by embedding and/or sectioning (such as knife marks and shatter) although slightly oblique sectioning could cause variations in wall thicknesses.

RESULTS

Our samples contain eight different populations identified as eukaryotes. At least two (*Tappania plana* and *Shuiyousphaerium macroreticulatum*) can be recognized as eukaryotic based on morphological characters observable by light microscopy. SEM imaging of cell wall microstructure marks two additional forms (*Satka favosa* and *Valeria lophostriata*) as protists. Our TEM investigation of these four first taxa shows that wall

Table 1 Species of Mesoproterozoic acritarchs from the Roper Group, Australia and the Ruyang Group, China; stratigraphic location, depth in core and facies distribution

Species	Stratigraphic location	Depth in core (m)	Facies
Tappania plana	Roper Group	GG1340.2	Distal shelf
Satka favosa	Roper Group	U6305.1	Marginal marine
		U6230.8	Marginal marine
Valeria lophostriata	Roper Group	U6305.1	Marginal marine
Leiosphaeridia crussu	Roper Group	GG1340.2	Distal shelf
		U6230.8	Marginal marine
		U6305.1	Marginal marine
L. tenuissima	Roper Group	GG1340.2	Distal shelf
		U6305.1	Marginal marine
L. jacutica	Roper Group	U6305.1	Marginal marine
Striated tubes	Roper Group	A82/3311.3	Inner shelf
		U5130.5	Inner shelf
Shuiyousphaeridium macroreticulatum	Ruyang Group	SYG 6 (outcrop)	Shelf

ultrastructure can be preserved for 1.5 billion years in eukaryotic microorganisms and, despite inevitable taphonomic modification, can still record different wall organizations reflecting the variety of their systematic relationships. However, for the four remaining taxa (three species of *Leiosphaeridia* and unnamed tubular microfossils) with simple morphologies, TEM imaging is necessary to reveal ultrastructures that support a eukaryotic affinity and not a cyanobacterial interpretation.

For the spheroidal acritarchs, preserved wall ultrastructures range from single, homogeneous, electron-dense layers of variable thickness – and variably ornamented – to multilayered walls differentiated by electron density and texture. Besides the obvious compression and folding of spheres, taphonomic variations included incomplete external wall layers for multilayered walls, perforations of less resistant layers, corrosion of surfaces, and variations in wall thicknesses due to compression. These variations, however, do not obscure the basic organization of wall ultrastructure characteristic of each species and recognizable in each specimen for at least some of its wall length. To the extent that diagenesis has influenced ultrastructure, then, it would appear have done so following the wall structures and chemistries that distinguished these organisms in life.

Tappania plana (Yin 1998) was first reported from Mesoproterozoic shales of the Ruyang Group, China (Yin, 1998), but recent discoveries from Australia (Javaux *et al.*, 2001), India (Prasad & Asher, 2001), and Russia (Sergeev, pers. comm. 2002) show that these protists ranged widely in Mesoproterozoic seaways. Tappania has broadly spheroidal vesicles of variable size (20–160 μm) that bear zero to 20 heteromorphic processes distributed asymmetrically about the vesicle surface (Yin, 1998; Javaux *et al.*, 2001).

Processes extend for varying distances from the vesicle (25–60 μm) and sometimes branch (long arrow in Fig. 2a). The processes communicate freely with the vesicle interior; SEM observations show structural continuity between the vesicle wall and the bases of processes (Fig. 2d). Vesicles may also bear up to three bulbous extensions, suggestive of budding (short arrow in Fig. 2a), and some vesicles bear neck-like extensions that could be excystment structures (arrow in Fig. 2b). The structures interpreted as possible buds are always closed hemispheric protrusions, and they can be as many as three on the same specimen. In contrast, the extensions interpreted as possible excystment structures flare outward, sometimes open at their distal extremity, and occur alone on specimens with no processes. The Roper population shows a high morphological diversity (Fig. 2a–c) that includes morphologies assigned to two different species in the Ruyang assemblage (*T. plana* and *T. tubata*, Yin, 1998). TEM images of *T. plana* show that its wall is single-layered, 144–456 nm thick, electron-dense, and homogeneous (Fig. 2e). Shatter marks are visible on Fig. 2(e) but these marks do not cause any artifacts that could contribute to the reported ultrastructure. Variations in wall thickness could be due to compaction.

As noted by Javaux *et al.* (2001, 2003), the irregular morphology and asymmetric distribution of processes in *Tappania* stand in marked contrast to the regular size and distribution of processes in most younger acritarchs and suggest that *Tappania* might have been an actively growing vegetative cell or germinating cyst rather than a metabolically inert spore (as commonly assumed for acritarchs; see also Butterfield *et al.*, 1994). To the best of our knowledge, *Tappania*'s combination of large size, preservable walls, complex processes, and possible excystment structures does not occur in Bacteria or Archaea. In eukaryotes, the kind of morphological remodeling necessary to account for the morphology of *Tappania* requires a dynamic cytoskeleton (Javaux *et al.*, 2001).

Valeria lophostriata Jankauskas (1989), is known from Mesoproterozoic and lower Neoproterozoic sedimentary successions on four continents (Hoffman & Jackson, 1996; Xiao *et al.*, 1997; Hoffman, 1999; Javaux *et al.*, 2001), and it has been recently discovered by us in late Palaeoproterozoic (CA. 1650 Ma) shales of the Mallapunyah Formation, northern Australia. *Valeria* is easily distinguished by its concentric striations observable by light microscopy (Fig. 2f). SEM observation shows these striations to consist of parallel ridges uniformly spaced one micron apart on the internal surface of the vesicle (Fig. 2g), strongly suggesting an eukaryotic affinity. Indeed, no prokaryotic organism is known to produce such regularly spaced micron-scale ornamentation on preservable acid-resistant walls. Ultrathin sections observed under TEM show a 177–296 nm thick, single-layered, homogeneous, electron-dense wall (Fig. 2h–i) with ridges. The irregularly spaced and sized holes in the wall show some degradation of the organic matter (Fig. 2i).

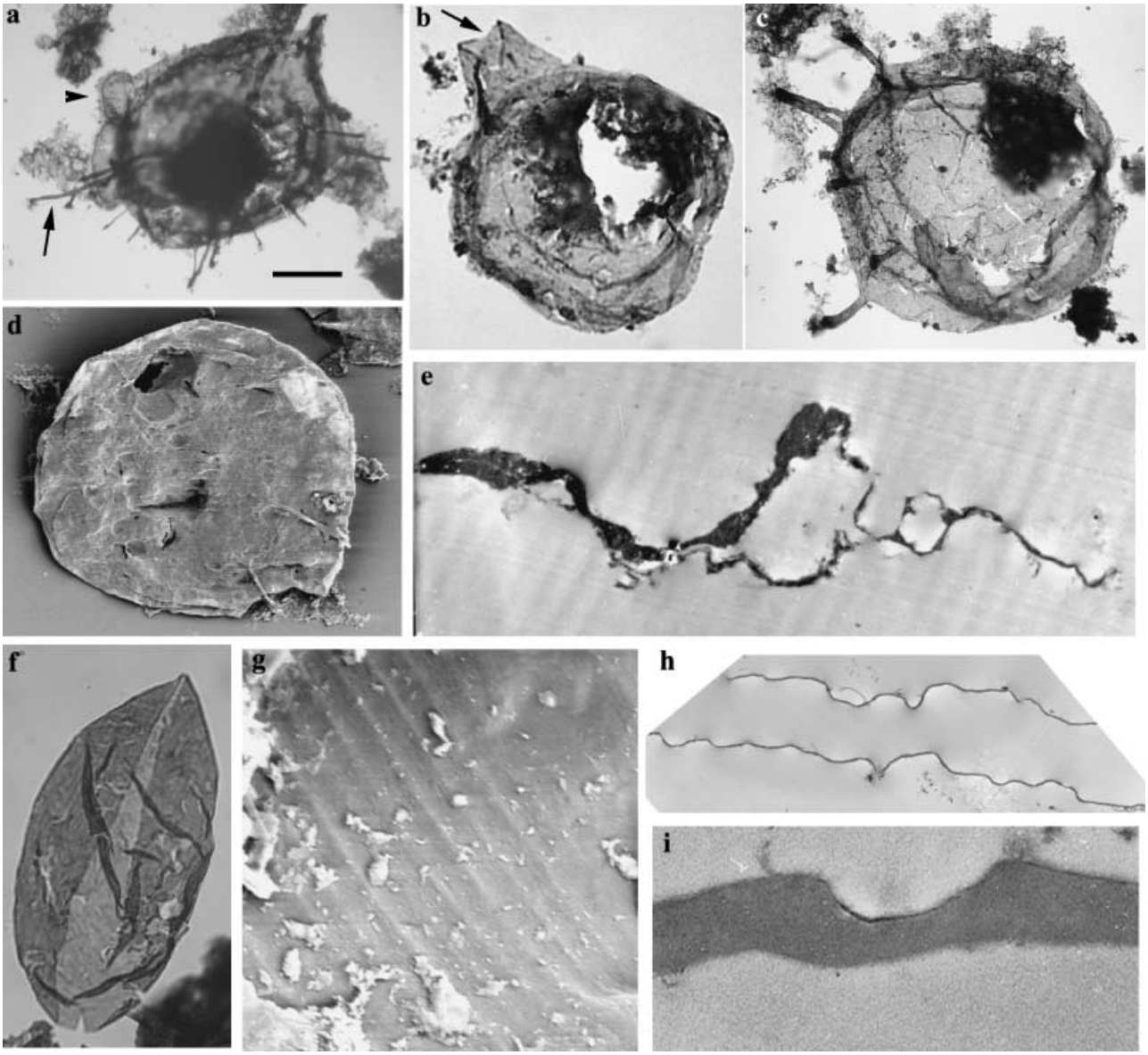

Fig. 2 Eukaryotic microfossils from the Roper Group, Australia. a–e: *Tappania plana*, a–c: light microscopy, a: specimen with heteromorphic processes (including a branched process-long arrow) distributed asymmetrically about the vesicle and budding (short arrow), b: specimen with possible excystment structure (arrow), c: specimen with asymmetrically distributed processes with closed, slightly expanded terminations, d: SEM showing structural continuity between vesicle wall and process bases, e: TEM showing unilayered homogeneous electron-dense wall with variable thickness due to taphonomic processes; f–i: *Valeria lophostriata,* f: partially enrolled half vesicle, likely resulting from medial split (light microscopy), g: SEM showing ridges spaced 1 μm apart on the internal surface of the vesicle, h, i: TEM showing two walls of compressed vesicle with ridges (h) and unilayered homogeneous electron-dense wall (i). Scale bar in a = 35 μm for a, 20 μm for b, 25 μm for c, 33.5 μm for d, 1.4 μm for e, 32 μm for f, 2.5 μm for g, 2 μm for h, 0.25 μm for i.

Satka favosa Jankauskas (1989), was initially discovered in Mesoproterozoic shales from the Southern Urals region of Russia (Jankauskas, 1989). Observed under the light microscope, its wall appears to be made of small plates (Figs 3a,b). SEM shows more clearly that the wall consists of polygonal plates up to 15 microns in maximum dimension that form a tessellated pattern (Figs 3c,d), a wall construction unknown in prokaryotes. The plates are polygonal building units and not incisions in the wall; they were commonly dissociated during burial compaction. The plates show some degradation of their surfaces (small fractures, corrosion) (Fig. 3d). TEM images of ultrathin-sections through preserved walls reveal 700 nm thick electron dense and homogeneous wall ultrastructure (Figs 3e,f). (Note that the wall structure of other species assigned to *Satka* does not closely resemble that of *S. favosa*; some of them, *S. squamifera* in particular, may be the preserved envelopes of cyanobacteria.). Knife marks (oblique white lines) are visible on Fig. 2(e).

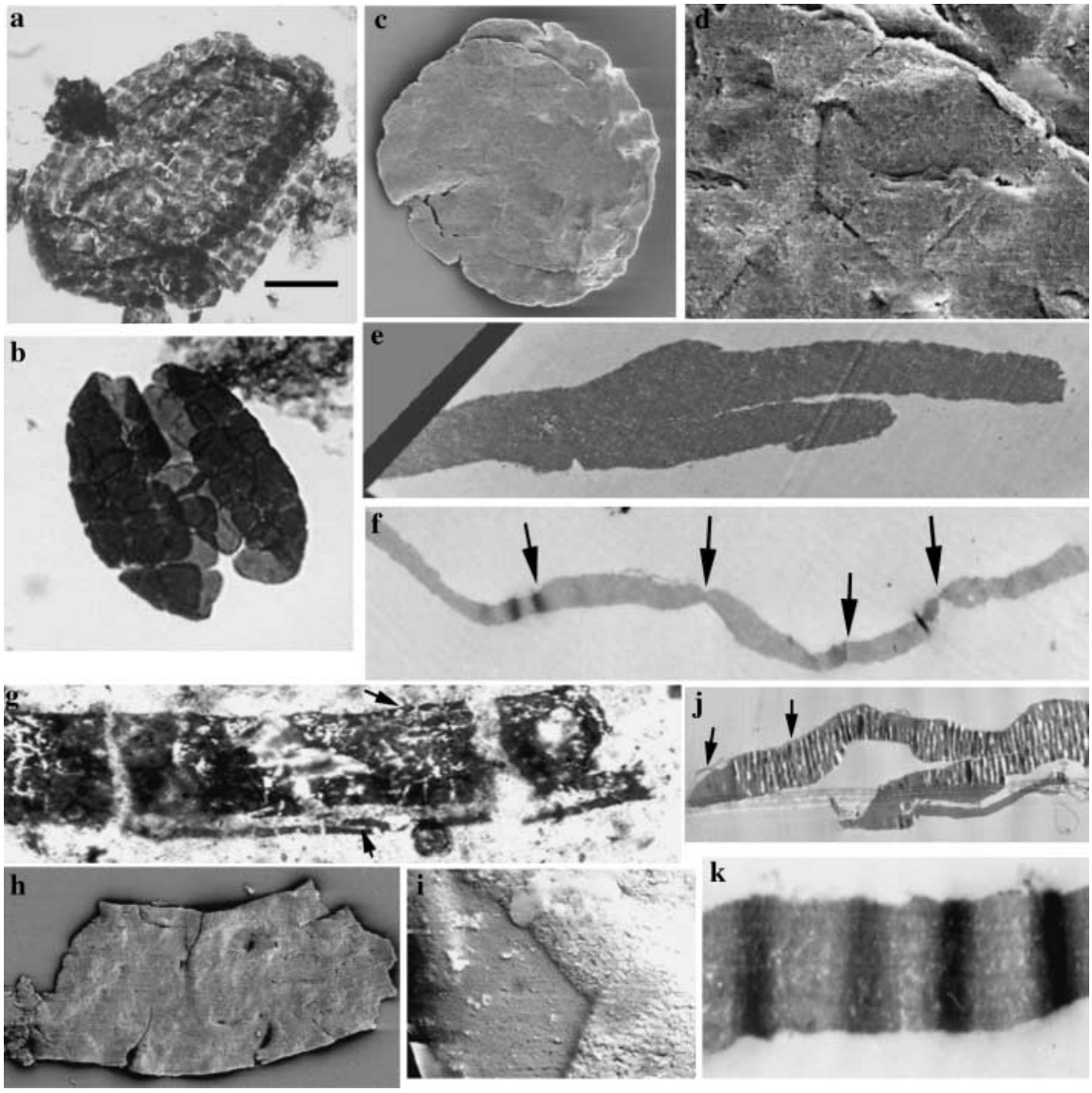

Fig. 3 Eukaryotic microfossils from the Roper Group, Australia. a–f: *Satka favosa*, a, b: specimens showing wall of polygonal plates sometimes detaching (Fig. 3b) (light microscopy), c, d: SEM showing whole specimen (Fig. 3c) and detail of juxtaposed polygonal plates (Fig. 3d), plate surfaces in d show some corrosion and cracks due to taphonomic processes, e, f: TEM showing unilayered homogeneous electron-dense wall with plate margins (arrows) (oblique lines in e are shatter marks); g–k: large striated tubes, g: specimen showing longitudinal striations (arrows) (light microscopy), h–i: SEM showing no striations but wall made of packed granules, j–k: TEM of transverse section showing fibrous wall ultrastructure (k) with alternating electron-dense and electron-tenuous bands, sometimes with external layer preserved (arrows in j), and variable wall thickness (j) due to oblique semithick sectioning through the two compressed walls of the tube (1 μm thick semithin section; other sections are 50–60 nm thick ultra-thin sections). Scale bar in a = 48 μm for a, 30 μm for b, g and h, 10 μm for c, 5 μm for d and f, 1 μm for e, 0.93 μm for i, 11.7 μm for j, 0.5 μm for k.

Large striated tubes occur abundantly in inner shelf shales of the Roper Group. The carbonaceous tubes are up to 150 μm in diameter and more than a millimeter long (Fig. 3g). Light microscopy shows longitudinal, micron-scale striations along the tubes (arrows in 3 g); SEM reveals layers of densely packed granules but does not show structures that could account for the longitudinal striations (Figs 3h,i). At the ultrastructural level, however, transverse sections of the wall show a clear alternation of electron-dense and electron-tenuous bands that correspond in size and distribution to the striations observed by light microscopy (Figs 3j,k). The striations, thus, reflect original compositional heterogeneities in the tube wall, indicating complex physiological controls on wall formation. The wall is about one μm thick and consists of layers of packed granules, as seen under SEM (Fig. 3i). In some individuals, an outer, electron-dense layer is preserved (arrows in Fig. 3j). Variations in wall thickness are due to oblique sectioning of the semithin (1 μm thick) section in Fig. 3(j). (Ultra-thin sections are about 50 nm thick).

The Roper tubes are broadly reminiscent of the cylindrical sheaths formed by (large) filamentous cyanobacteria and sulphur-oxidizing bacteria. The sheaths of modern cyanobacteria and S-oxidizing bacteria, however, share an ultrastructure characterized by fibrous layers (Hoiczyk & Hansel, 2000); neither is known to produce features akin to the compositional striations observed in the fossil population. The Roper tubes also differ from other tubular fossils described in the late Precambrian and Cambrian (e.g. *Marpolia*, vendotaenids) by their strong corduroy-like striations.

Leiosphaerids (simple organic-walled spheres) are common in carbonaceous shales deposited through most of the Proterozoic Eon. Palaeontological investigations of these fossils have largely been restricted to light microscopy, with different species arbitrarily distinguished on the basis of size and inferred wall thicknesses (Jankauskas, 1989). Previous TEM studies of leiospheres, however, suggest that ultrastructure may provide a firmer basis for distinguishing different populations. Some leiospheres preserve a multilayered wall similar to chlorococcalean green algae (Arouri *et al.*, 1999), while others reveal a single-layered, homogeneous wall (Peat, 1981; Arouri *et al.*, 2000; Talyzina & Moczydlowska, 2000), or a homogenous wall perforated by pore canals similar to some prasinophyte green algae (Loeblich, 1970). TEM of Roper leiosphaerids populations not only corroborates differences observed via light microscopy, but suggests that they represent distinct clades, implying a level of taxonomic diversity undetected by optical investigation.

Leiosphaeridia jacutica (Jankauskas 1989), is a thick-walled sphere with coarse folds, a diameter greater than 70 μm (Figs 4a,b) and a smooth to granulate surface at the SEM level (Fig. 4b). TEM observation shows that the 1.6–2.5 μm thick wall contains two 0.2–0.4 μm electron-dense, homogeneous layers that sandwich a 1.2–1.7 μm thick central layer with an electron-dense, porous texture (Figs 4c,d,m). This porosity could be due to degradational perforations of the less resistant organic layer. In rare cases, an outer layer of intermediate electron density is preserved (arrow in Fig. 4d). Degradation during fossilization and/or possibly during acid maceration probably removed this thin organic layer in most specimens.

Leiosphaeridia crassa (Jankauskas 1989), is similar in general morphology to *L. jacutica*, but is smaller (<70 μm) (Figs 4e,f) and has a smooth surface at the SEM level (Fig. 4f). Its wall ultrastructure, however, is fundamentally different, consisting of a thin multilayered wall (80–150 nm) in which two electron-tenuous amorphous layers surround an electron-dense homogeneous layer (Figs 4g–i,n,o), with a possible, rarely preserved trilaminar structure (TLS) consisting of two electron-dense layers around a thicker electron-tenuous layer (arrows in Figs 4i,o). The wall ultrastructure is obscured at various areas of its length by irregular darkening (coalification) so that the possible TLS structure is scarcely visible. Arouri *et al.* (1999) also reported partial preservation of TLS structure in Neoproterozoic acritarch walls. Locally, inner and outer walls are joined together (arrow in Fig. 4h). The coarse folds seen at light microscopy are due to a rigid wall rather than to its thickness, as it was previously assumed. TLS structures occur in the acetolysis-resistant walls of many green algae (Gelin *et al.*, 1999). Roper populations of *L.* crassa could be green algae, although this remains to be confirmed by microchemical analysis, currently underway.

Leiosphaeridia tenuissima (Jankauskas 1989*),* is a less rigid, thin-walled sphere, 30–80 μm in diameter, with thin folds (Figs 4j,k) and a smooth surface at the SEM level (Fig. 4k). At the ultrastructural level, its wall is multilayered, 177–414 nm thick, and consists of a thin electron dense layer that caps an outer 60 nm thick medium-dense porous layer, an intermediate 355 nm thick electron-dense fibrous layer with fibers parallel to the vesicle surface, and an inner electron-tenuous amorphous layer (Figs 4l,p).

Shuiyousphaeridium macroreticulatum (Yan, 1992*)*, is an acanthomorphic protist preserved in shales of the Mesoproterozoic Ruyang Group, northern China. It has the most highly ornamented wall of any known Mesoproterozoic fossil, and, indeed, it is more ornate than most Neoproterozoic acritarchs. The large (100–250 μm) spheroids have a reticulated surface and numerous regularly spaced cylindrical processes that flare outward (Fig. 5a–d). SEM images show that the wall's outer surface is covered with ridges that delimit granular polygonal fields (Fig. 5f); inner wall surfaces show the reverse of the same ornamentation – closely packed, beveled hexagonal plates (2 μm across; Figs 5g,i). TEM images show that the c. 1.5 μm wall is multilayered. A 391–586 nm thick, electron-dense, homogeneous layer of organic plates lies between an outer layer of debris and sectioned processes and a thin electron-tenuous layer that lines the inner side of the plates (Figs 5h,i,j). Note that the width of plates seen in TEM could be larger than that measured in SEM, due to oblique sectioning through the hexagonal plates. Oblique lines in Figs 5(h),(j) are shatter marks.

Recognizing and interpreting the fossils of early eukaryotes

Morphologically preserved fossils can be identified as eukaryotic based on a number of features thought to be diagnostic of the domain (Javaux *et al.*, 2003). These include: (1) wall structure and surface ornamentation (2) processes that extend from vesicle walls (3) excystment structures (openings through which cysts liberate their cellular contents) (4) wall ultrastructure and (5) wall chemistry. Although most eukaryotic cells are larger than 10–20 μm in diameter, while most Bacteria and Archaea are no more than 1–2 μm in maximum dimension, the discovery of abundant 1–2 μm picoeukaryotes (Moreira & Lopez-Garcia, 2002) and 750 μm sulphur bacteria (Schulz *et al.*, 1999), as well as 30–50 μm cyanobacterial envelopes (Waterbury & Stanier, 1978) show that within the range commonly exhibited by Proterozoic

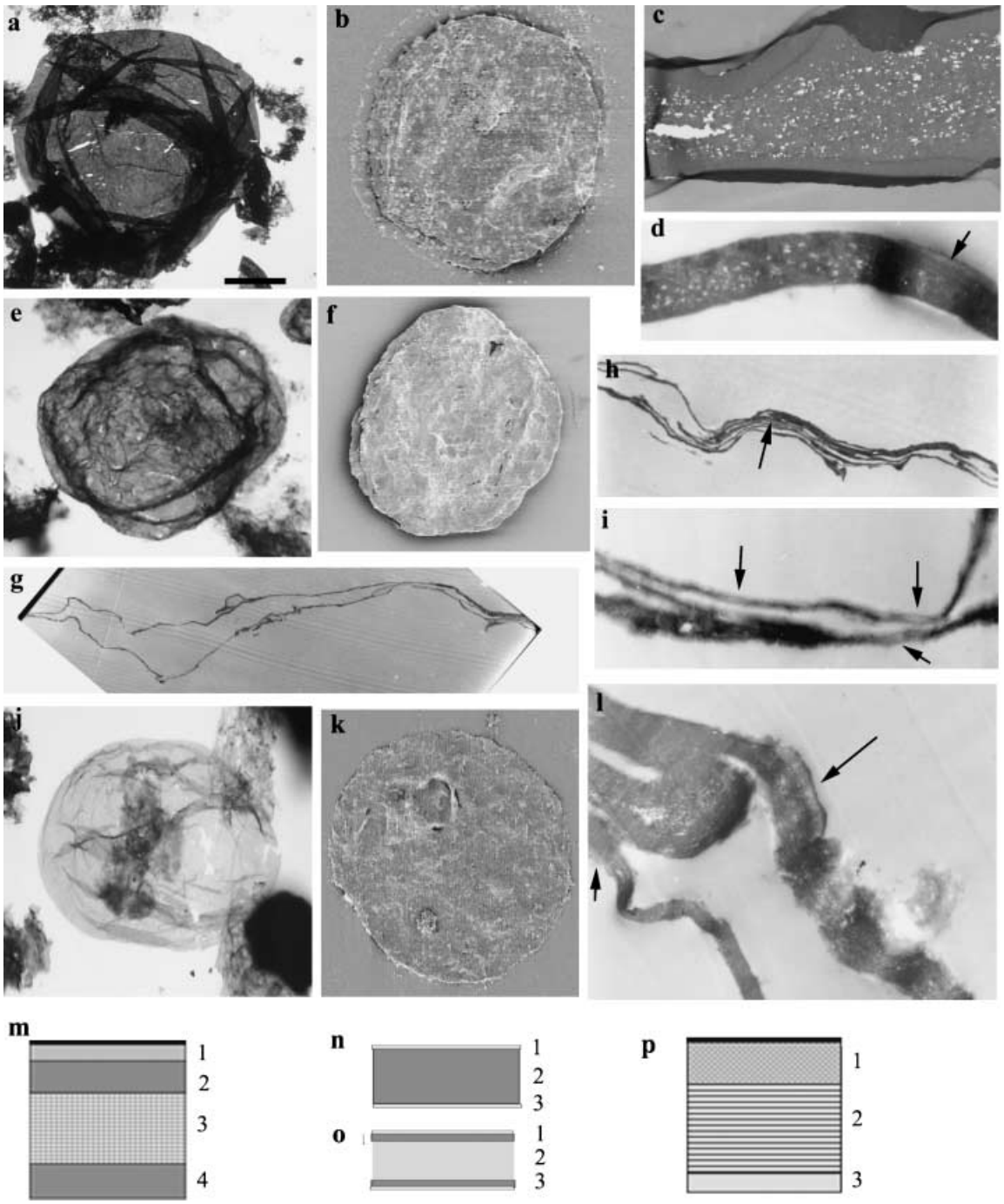

Fig. 4 Leiosphaerids from the Roper Group, Australia. a–d, m: *Leiosphaeridia jacutica*. a: specimen showing thick folds (light microscopy), b: SEM showing a smooth to granulate surface c–d: TEM showing a multilayered wall ultrastructure of two electron-dense, homogeneous layers (2, 4 in m) that sandwich a thick central layer with electron-dense, porous texture (3 in m) (possibly degradational perforations); sometimes an outer medium-dense layer is preserved (1 in m, arrow in d), m: diagram of wall ultrastructure; e–i, n–o: *Leiosphaeridia crassa*. e: light microscopy, f: SEM showing a smooth surface, g: TEM showing two walls of compressed acritarch, h: TEM showing locally attached inner walls/membranes (arrow), I: TEM showing ultrastructure of each wall consisting of two electron-tenuous amorphous layers (1, 3 in n) surrounding a electron-dense homogeneous layer (2 in n) with a possible, rarely preserved trilaminar structure (TLS) of two electron-dense layers (1, 3 in o) around a thicker electron-tenuous layer (2 in o, arrows in i); n–o: diagram of wall ultrastructure without (n) and with (o) TLS layer; j–l, p: *Leiosphaeridia* tenuissima, j: specimen showing wall with thin folds (light microscopy), k: SEM showing a smooth surface, l: TEM showing two multilayered walls of compressed *acritarch* folding inward (upper left side of l) consisting of a thin electron dense layer capping an outer medium-dense porous layer (1 in p), an intermediate electron-dense fibrous layer with fibers parallel to vesicle surface (2 in p), and an inner electron-tenuous amorphous layer (3 in p), external layers often removed by degradation (arrows show locally preserved layers), p: diagram of wall ultrastructure. Scale bar in a = 30 μm for a, 50 μm for b, 1 μm for c, 1.7 μm for d, 10 μm for e and f, 5 μm for g, 0.8 μm for h, 0.3 μm for i and 30 μm for j and k, and 1.6 μm for l.

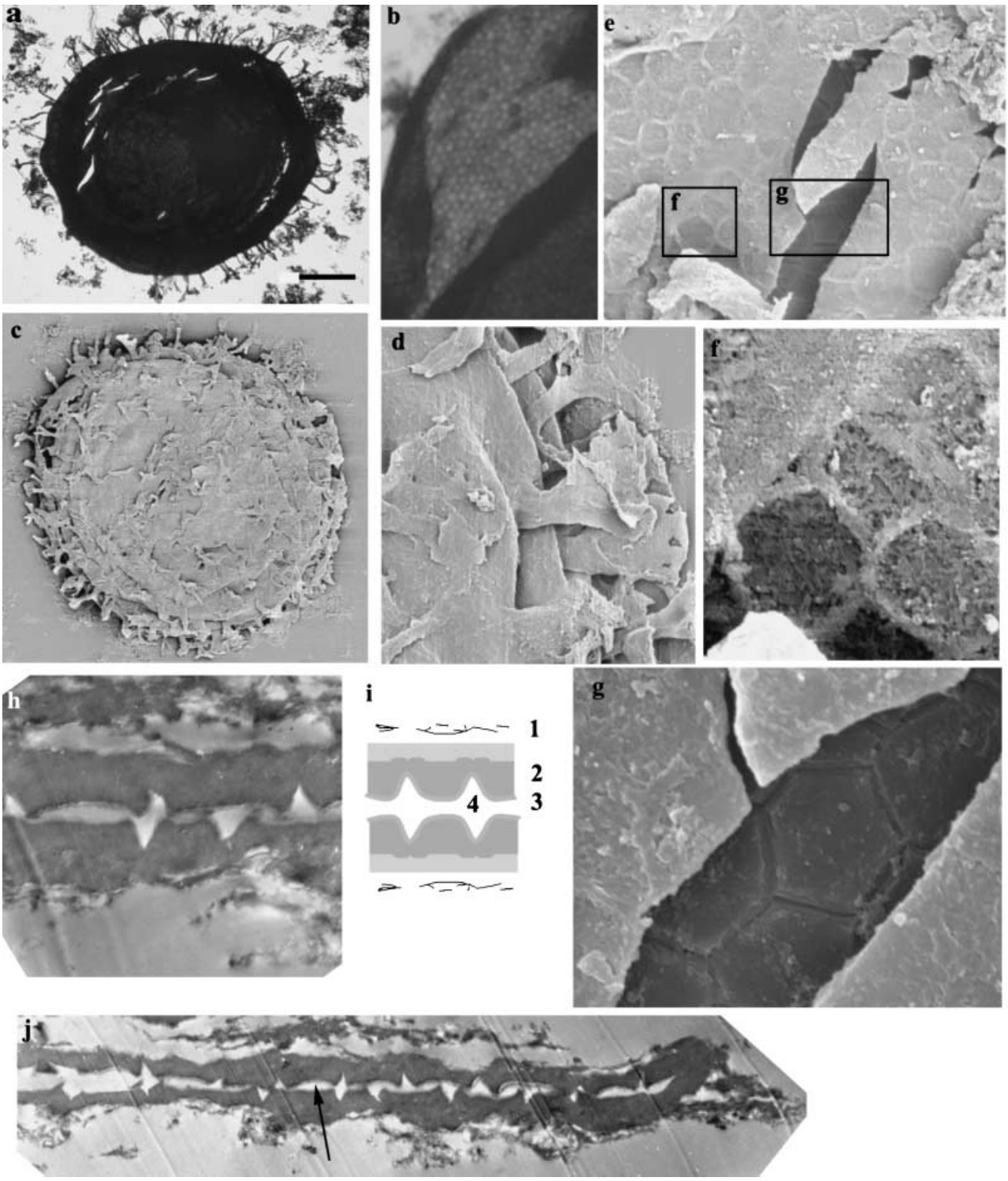

Fig. 5 *Shuiyousphaeridium macroreticulatum* from the Ruyang Group, northern China. a, b: light photographs showing specimen with numererous regularly spaced cylindrical processes that flare outward (a) and a reticulated surface (b), c–g: SEM showing whole specimen (c), detail of flaring furcating processes (d), wall reticulation (e), outer wall surface covered with ridges that delimit granular polygonal fields (f), and inner wall surface of closely packed, beveled hexagonal plates (g), h, j: TEM showing the two walls of compressed acritarch (j) and multilayered wall comprising a thick electron-dense homogeneous layer of organic plates (2 in i) surrounded by an outer layer (1 in i) of debris and processes and a thin electron-tenuous layer that lines the inner side of plates (3 in i), aroow in j shows the central cavity of the vesicle (4 in i) i: diagram of ultrastructure (1: debris and sectioned processes, 2: plates with outer ridges and inner incisions, 3: inner lining of the plates, 4: vesicle internal space). Note that width of plates seen in TEM could be larger than that measured in SEM, due to oblique sectioning through the hexagonal plates. Oblique lines in h and j are shatter marks. Scale bar in a = 50 μm for a and c, 13 μm for b, 10 μm for d, 2.5 μm for e, and 1 μm for f and g.

fossils, cell size is not sufficient to differentiate prokaryotic from eukaryotic microfossils. Prokaryotic organisms can synthesize both cell wall ornament and preservable structures; however, wall ornamentation rarely occurs on the size scale observed in Proterozoic fossils and is seldom found on preservable structures (Javaux *et al.*, 2003).

Resting cells and reproductive cysts of many protists display micron-scale patterns of lineations, fields, spines or bosses not known among prokaryotic organisms. Some prokaryotic cells are ornamented with concentric rings of juxtaposed filaments, or fibrils, pili and fimbriae, but these features occur at the nanoscale (Boone & Castenholz, 2001), not the microscale seen in Roper acritarchs. Moreover, this type of proteinaceous surface ornamentation would probably not be preserved since it is easily removed by chemicals and lost in cultures, and easily degraded under diagenetic conditions. Some cyanobacteria, myxobacteria and filamentous sulphur bacteria can produce large bacterial structures but none of those are ornamented. Cyanobacterial sheaths are preserved in the fossil record, in preference to the peptidoglycan-rich cell walls, as shown by taphonomic experiments (Bartley, 1996). The 'F layer' of pleurocapsalean cyanobacteria, an outer wall layer composed of fibrils, is generally up to about 1 μm thick, but wall thickness varies, as the layer continues to expand as its enclosed cell increases in size (Waterbury & Stanier, 1978). The 'F layer' is distinct from the fibrous layer described for *Leiosphaeridia tenuissima*, where long fibers run parallel to the wall surface; nor does it closely resemble the multilayered walls, including nonfibrous layers, observed in other Roper populations (see above). However, it is unknown if the wall of other bacteria (with morphologies comparable to the studied microfossils) would withstand fossilization and the acid maceration used to extract organic-walled microfossils from shales.

Neoproterozoic and Palaeozoic acritarchs with wall ornamentation are ascribed to eukaryotes with confidence. Roper microfossils do not display the strong ornamentation seen in some younger populations. Nonetheless, the ornamentation and wall structure of some Roper taxa identify them as protists. Ruyang microfossils display clearly eukaryotic morphology; as Cavalier-Smith, (2002) pointed out, 'cysts with spines or reticulate surface sculpturing would probably have required both an endomembrane system and a cytoskeleton, the most fundamental features of the eukaryotic cell, for their construction'.

CONCLUSIONS

TEM observations of wall ultrastructure extend our view of Mesoproterozoic biology, identifying a moderate diversity of microfossil populations as eukaryotic and implying that preserved fossils derive from a number of distinct clades, a conclusion that could not have been drawn using light microscopy alone. Microchemical analyses of single acritarchs (ongoing) will help refine the biological affinities of these early eukaryotes.

Despite the growing inventory of protists in the Roper, Ruyang, and a few other exceptionally preserved fossil assemblages, however, the observed diversity of Mesoproterozoic eukaryotes remains below known Neoproterozoic levels. The general pattern of low Mesoproterozoic and moderate Neoproterozoic diversity, with a burst of new micro- and macrofossil forms near the end of the eon (Knoll, 1994; Vidal & Moczydlowska, 1997; Xiao *et al.*, 2002) still seems to hold, although the degree to which this pattern mainly reflects the initial phylogenetic divergence of the Eucarya, as opposed to expanding environmental opportunity (Anbar & Knoll, 2002), no longer seems so clear. Morphologically complex protistan fossils are currently unknown from rocks older than *c.* 1650 Ma, but simple leiospherid acritarchs occur in successions that stretch back toward the beginning of the Proterozoic Eon (Sun & Zhu, 1998). The challenge is now to characterize the ultrastructure of these remains with the goal of tracing the early history of eukaryotic diversification.

ACKNOWLEDGEMENTS

This paper is a contribution to the Australian Geological Survey Organization's NABRE project. We thank J. Jackson and P. Southgate for helpful discussions and advice on sampling of the Roper Group; S. Xiao for the Ruyang Group samples, and L. Kerr for technical help with TEM (MBL). Yin provided helpful information on Chinese stratigraphy, V. Sergeev on Russian palaeontology, and J. Waterbury on cyanobacteria. We thank S. Xiao and M. Moczydlowska-Vidal, and two unidentified reviewers for helpful comments. Research supported by NASA Exobiology Grant NAG5-3645, the NASA Astrobiology Institute, the Australian Research Council and Macquarie University and the Belgian Federal Science Policy office return grant.

REFERENCES

Abbott ST, Sweet IP (2000) Tectonic control on third-order sequences in a siliciclastic ramp-style basin: an example from the Roper Superbasin (Mesoproterozoic), northern Australia. *Australian Journal of Earth Sciences* **47**, 637–657.

Amard B (1992) Ultrastructure of *Chuaria* (Walcott) Vidal and Ford (Acritarcha) from the Late Proterozoic Pendjari Formation, Benin and Burkina-Faso, West Africa. *Precambrian Research* **57**, 121–133.

Anbar AD, Knoll AH (2002) Proterozoic ocean chemistry and evolution: a bioinorganic bridge? *Science* **297**, 1137–1142.

Arouri K, Greenwood PF, Walter MR (1999) A possible chlorophycean affinity of some Neoproterozoic acritarchs. *Organic Geochemistry* **30**, 1323–1337.

Arouri K, Greenwood PF, Walter MR (2000) Biological affinities of Neoproterozoic acritarchs from Australia: microscopic and chemical characterization. *Organic Geochemistry* **31**, 75–89.

Bartley JK (1996) Actualistic taphonomy of Cyanobacteria: implications for the Precambrian fossil record. *Palaios* **11**, 571–586.

Batten (1996) *Palynofacies and Petroleum Potential*. In: Jansonius, J, & McGregor, DC, eds. Palynology, principles and applications,

Vol. 3 *Am. Ass.* of *Stratigraphic Palynologists Foundation*, 26, 1065–1084.
Brocks JJ, Logan GA, Buick R, Summons RE (1999) Archean molecular fossils and the early rise of eukaryotes. *Science* **285**, 1033–1036.
Butterfield NJ (2000) *Bangiomorpha pubescens* n. General, n.sp. implications for the evolution of sex, multicellularity and the Mesoproterozoic/Neoproterozoic radiation of eukaryotes. *Paleobiology* **26**, 386–404.
Butterfield NJ (2004) A Vaucherian alga from the middle Neoproterozoic of Spitsbergen: implications for the evolution of Proterozoic eukaryotes and the Cambrian explosion. *Paleobiology* **30**, 231–252.
Butterfield NJ, Knoll AH, Swett K (1994) Paleobiology of the Neoproterozoic Svanbergfjellet Formation, Spitsbergen. *Fossils Strata* **34**, 1–84.
Cavalier-Smith T (2002) The neomuran origin of archaebacteria, the negibacteria root of the universal tree and bacteria megaclassification. *International Journal of Systematic Microbiology* **52**, 7–76.
Garrity G (ed) (2001) *Bergey's Manual of Systematic Bacteriology: 2001*, Vol. 1: the Archea and the Deeply Branching and Phototrophic Bacteria, 2nd edn. Springer N.Y., USA. 1721.
Gelin F, Volkman JK, Largeau C, Derenne S, Sinninghe Damste JS, De Leeuw JW (1999) Distribution of aliphatic, nonhydrolyzable biopolymers in marine microalgae. *Organic Geochemistry* **30**, 147–159.
Grey K (1999) A modified palynological preparation technique for the extraction of large Neoproterozoic acanthomorph acritarchs and other acid insoluble microfossils. *Geological Survey of Western Australia*, **Record 199/10**, 1–23.
Hoffman HJ (1999) Global distribution of the Proterozoic sphaeropmorph acritarch *Valeria lophostriata* (Jankauskas). *Acta Micropaleontologica Sinica* **16**, 215–224.
Hoffman HJ, Jackson GD (1996) Notes on the geology and paleontology of the Thule Group, Ellesmere Islands, Canada and North-West Greenland. *Geological Survey of Canada Bulletin* **495**, 1–26.
Hoiczyk E, Hansel A (2000) Cyanobacterial cell walls: news from an unusual prokaryotic envelope. *Journal of Bacteriology* **182**, 1191–1199.
House CH, Fitz-Gibbon ST (2002) Using homolog groups to create a whole-genomic tree of free-living organisms: An update. *Journal of Molecular Evolution* **54**, 539–547.
Jankauskas TV (1989) *Mikrofossilii dokembriya SSSR* (Precambrian microfossils of the USSR). *Nauka Leningrad*, 1–190.
Javaux EJ, Knoll AH, Walter MR (2001) Morphological and ecological complexity in early eukaryotic ecosystems. *Nature* **412**, 66–69.
Javaux EJ, Knoll AH, Walter MR (2003) Recognizing and Interpreting the Fossils of Early Eukaryotes. *Origins of Life and Evolution of the Biosphere* **33** (1), 75–94.
Jux U (1968) Uber den Feinbau der Wandung bei *Tasmanites* Newton. *Palaeontographica Abt. B* **124**, 112–124.
Jux U (1971) Uber den Feinbau der Wandungen einiger paläozoischer Baltisphaeidiacean. *Palaeontographica Abt. B* **136**, 115–128.
Jux U (1977) Uber die wandstrukturen sphaeromorpher acritarchen: *Tasmanites* Newton, *Tapajonites* Sommer & Van Boekel, *Chuaria* Walcott. *Palaeontographica Abt. B* **160**, 1–16.
Kjellström G (1968) Remarks on the chemistry and ultrastructure of the cell wall of some Palaeozoic leiospheres. *Geologiska Föreningens I Stockholm Förhandlingar* **90**, 118–221.
Knoll AH (1992) the early evolution of eukaryotes – a geological perspective. *Science* **256**, 622–627.
Knoll AH (1994) Proterozoic and early Cambrian protists – evidence for accelerating evolutionary tempo. *Proceedings of the National Academy of Sciences* **91**, 6743–6750.
Knoll AH, Calder S (1983) Microbiota of the Late Precambrian Ryssö Formation, Nordaustlandet, Svalbard. *Palaeontology* **26**, 467–496.
Kralik M (1982) Rb-Sr age determinations on Precambrian carbonate rocks of the Carpentarian McArthur Basin, Northern Territory, Australia. *Precambrian Research* **18**, 157–170.
Loeblich TR (1970) Morphology, ultrastructure and distribution of Palaeozoic acritarchs. *Proceedings of the North American Palaeontological Convention G.* 705–788
Martin F, Kjellström G (1973) Ultrastructural study of some Ordovician acritarchs from Gotland, Sweden. *Neues Jahrb Geological Paläontological Monatsh* **1**, 44–54.
Moreira D, Lopez-Garcia P (2002) The molecular ecology of microbial eukaryotes unveils a hidden world. *Trends in Microbiology* **10** (1), 31–38.
Oehler DZ (1977) Pyrenoid-like structures in Late Precambrian algae from the Bitter Springs Formation of Australia. *Journal of Paleontology* **51**, 885–901.
Pace NR (1997) A molecular view of microbial diversity and the biosphere. *Science* **276**, 734–740.
Page RW, Jackson MJ, Krasay AA (2000) Constraining sequence stratigraphy in north Australian basins: SHRIMP U-Pb zircon chronology between Mt. Isa and McArthur River. *Australian Journal of Earth Sciences* **47**, 431–459.
Pearson A, Budin M, Brocks J (2003) Phylogenetic and biochemical evidence for sterol synthesis in the bacterium Gemmata obscuriglobus. *Proceedings of the National Academy of Sciences* **100**, 15352–15357.
Peat CJ (1981) Comparative light microscopy, scanning electron microscopy and transmission electron microscopy of selected organic walled microfossils. *Journal of Microscopy* **122**, 287–294.
Porter SM, Meisterfeld R, Knoll AH (2003) Vase-shaped microfossils from the Neoproterozoic Chuar Group, Grand Canyon: a classification guided by modern testate amoebae. *Journal of Paleontolology* **77**, 205–225.
Prasad B, Asher R (2001) Acritarch biostratigraphy and lithostratigraphic classification of Proterozoic and Lower Paleozoic sediments (Pre-Unconformity Sequence) of Ganga Basin, India. *Paleontographica Indica* **5**, 1–151.
Schulz HN, Brinkhoff T, Ferdelman TG, Marine MH, Teske A (1999) Dense populations of a giant sulfur bacterium in Namibian shelf sediments. *Science* **284**, 493–495.
Steiner M (1997) *Chuaria circularis* Walcott 1899- « Megasphaeromorph Acritarch » or Prokaryotic colony ? *Acta Universitatia Carolinae Geologica* **40**, 645–665.
Summons RE, Powell TG, Boreham CJ (1988) Petroleum geology and geochemistry of the Middle Proterozoic McArthur Basin, Northern Australia. III. Composition of extractable hydrocarbons. *Geochemica Cosmochemica Acta* **51**, 3075–3082.
Sun SF, Zhu SX (1998) Discovery of micropaleophytes from the Doucun subgroup (about 2400 Ma), Hutuo Group of Wutai Mountain. *Acta Micropaleontologica Sinica* **15** (3), 286–293.
Talyzina NM (2000) Ultrastructure and morphology of *Chuaria cir*cularis (Walcott, 1899) Vidal and Ford (1985) from the Neoproterozoic Visingso Group, Sweden. *Precambrian Research* **102**, 123–134.
Talyzina NM, Moczydlowska M (2000) Morphological and ultrastructural studies of some acritarchs from the Lower Cambrian Lukati Formation, Estonia. *Review of Palaeobotany and Palynology* **112**, 1–21.

Vidal G, Moczydlowska M (1997) Biodiversity, speciation, and extinction trends of Proterozoic and Cambrian phytoplankton. *Paleobiology* **23**, 230–246.

Waterbury JB, Stanier RY (1978) Patterns of growth and development in Pleurocapsalean cyanobacteria. *Microbiological Review* **42**, 2–44.

Xiao S, Knoll AH, Kaufman AJ, Yin L, Zhang Y (1997) Neoproterozoic fossils in Mesoproterozoic rocks? Chemostratigraphic resolution of a biostratigraphic conundrum from the North China Platform. *Precambrian Research* **84**, 197–220.

Xiao S, Yuan X, Steiner M, Knoll AH (2002) Macroscopic carbonaceous compressions in a terminal Proterozoic shales: a systematic reassessment of the Miaohe biota, South China. *Journal of Paleontology* **76**, 347–376.

Yin L (1998) Acanthomorphic acritarchs from Meso-Neoproterozoic shales of the Ruyang Group, Shanxi, China. *Review of Palaeobotany and Palynology* **98**, 15–25.